

## Adsorption of atenolol on nanostructured clays: Experimental Design, and Kinetic Study

Gabriel Santos da Rosa<sup>a</sup>, Daniel Moro Druzian<sup>b</sup>, Leandro Rodrigues Oviedo<sup>c</sup>, Alencar Kolinski Machado<sup>d</sup>, William Leonardo Da Silva<sup>e\*</sup>

Franciscan University (UFN), <sup>a</sup>Email: gabriel.srosa@ufn.edu.br; <sup>b</sup>Email: daniel.druzian@ufn.edu.br; <sup>c</sup>leandro.roviedo@gmail.com; <sup>d</sup>alencar.machado@ufn.edu.br; <sup>e</sup>Email: w.silva@ufn.edu.br, Santa Maria-RS ZIP:97010491, Brazil

### Abstract

The quality and quantity of water resources are fundamental aspects of sustainable development, and it is necessary to combine efficient water treatment technologies capable of eliminating and removing persistent contaminants especially the atenolol (AtL). In this sense, the present work aims to synthesize and characterize zeolites by sol-gel and hydrothermal methods from the rice husk and residual sludge and to apply in the removal of the AtL drug. In this sense, the adsorption was carried out in a batch system for 180 min, followed by initial AtL adsorption tests, and an experimental design. The characterizations confirmed the synthesis of zeolites with aluminosilicate phases (Metahalloysite (29.8 nm), Faujasite (14.2 nm), and Sodalite (17.5 nm)) and negative surface charge (-24.6, -26.4, and -18.8 mV). Moreover, the initial AtL adsorption tests indicated that sodalite (nSod) presented a higher removal of 82.5% of AtL compared to activated carbon of 42.8%. The experimental design using nSod indicated that variable adsorbent concentration and solution pH positively influenced the removal of AtL. The data from the kinetic studies demonstrated the formation of chemical bonds, where the pseudo-second-order model ( $q_e=28.68 \text{ g mg}^{-1} \text{ g}^{-1}$ ) best fitted the data. Therefore, it was possible to synthesize nanostructured zeolites of different phases with great potential for application in the removal of AtL.

**Keywords:** Adsorption; Drugs; Nanomaterials; Organic pollutants.

### 1. Introduction

The quality and quantity of water resources is a fundamental aspect of sustainable development. Thus, it is necessary to design and evaluate efficient water treatment technologies capable of eliminating, and removing persistent contaminants present in effluents and denoting factors that are economical, sustainable and environmentally friendly [1].

In this sense, one of the biggest problems are the persistent organic pollutants (e.g., atenolol - AtL), which are difficult to detect and classified as stable and toxic due to the properties including low biodegradability and bioaccumulation in aquatic organisms, requiring advanced treatments particularly adsorption, and heterogeneous photocatalysis [2]. Additionally, the AtL is rapidly absorbed by the human body (around 50% of the dose is absorbed and the remainder is expelled through urine) and can be found in Wastewater Treatment Plant (WWTPs), and sewage. It is worth mentioning that this pollutant is not yet controlled by Brazilian legislation and is present in several environmental matrices [3].

The use of advanced water treatment processes (e.g., adsorption, advanced oxidative processes and

membrane separation) are one of the ways to remedy this type of pollutant highlighting the use of nanostructured clay minerals that can increase the efficiency of the process [4].

About the clay minerals, Zeolites (ZO) are micro and macroporous structures made up of groups of aluminates and silicates, being a promising material for adsorbents due to the homogeneity of the pores making the processes extremely selective [5].

The (agro)industrial waste is a major socio-environmental problem, with most of which is disposed of incorrectly making it an environmental liability especially the rice husks around  $600 \times 10^3$  tons per year, and residual sludge around  $650 \times 10^3$  tons per year [6].

In this context, the present work aims to synthesize and characterize a nanostructured clay mineral from agro-industrial waste (rice husk and residual sludge from a water treatment plant) for the AtL adsorption correlating nanotechnology and sustainable development.

### 2. Materials and Methods

#### 2.1. Synthesis of the metahalloysite-nanozeolite

The sol-gel method [7] was used for the zeolite Metahalloysite (nMeta) production. Thus, 4 mL of

Tetraethyl orthosilicate ( $\text{SiC}_8\text{H}_{20}\text{O}_4$ , 99%, Sigma-Aldrich®) and 0.645 g of treated rice husk were mixed with 100 mL of absolute ethyl alcohol ( $\text{C}_2\text{H}_6\text{O}$ , 95%, Vetec®) under magnetic stirring (200 rpm for 20 min). The nitric acid ( $\text{HNO}_3$ , 98%, Synth®) was used for hydrolysis of the components making the solution with a pH around 2-3 mixed for 30 min. Moreover, the 2.150 g of the alumina source from a water treatment plant (calcined at 673.1 K) was added to the mix for 20 min. Subsequently, the sodium hydroxide ( $\text{NaOH}$ , 99%, Synth®) was added for the condensation process resulting in the increase of the pH solution to around 9-10. Finally, the sample was dried (343.1 K for 720 min) and calcined at 673.1 K for 120 min with a heating rate of 283.1 K  $\text{min}^{-1}$ .

## 2.2 Synthesis of the sodalite and faujasite nanozeolites

Sodalite (nSod) and Faujasite (nFau) nanozeolites were synthesized by the hydrothermal method [8] from (agro)industrial waste as precursors. Thus, 2.15 g of  $\text{Al}_2\text{O}_3$  and 0.68 g of  $\text{SiO}_2$  were diluted in 60 mL of 2 mol  $\text{L}^{-1}$   $\text{NaOH}$  (99%, Synth®) under magnetic stirring (120 rpm) at  $323.1 \pm 2$  K for 20 min. Subsequently, the mixture was transferred to a reaction in a stainless-steel autoclave lined with polytetrafluoroethylene (PTFE) heated in the conditions: Sodalite 453.1 K for 240 min and Faujasite 3613.1 K for 600 min. The nanozeolites were washed and dried in an oven at 353.1 K for 720 min.

## 2.3 Characterization of nanozeolites

The crystalline phases were identified by XRD in a Bruker diffractometer (D2 Advance model ( $\lambda_{\text{Cu-}\alpha}$  = 1.532 Å) with acceleration voltage and current of 30 kV and 30 mA, respectively, and Bragg angle ranging from 5° to 70°. The Bragg and Debye-Scherrer equations were used to determine the interplanar distance ( $d$ ), and average crystallite size ( $d_c$ ), according to the Equation (1)–(2), respectively. Furthermore, the database was used JCPDS (Joint Committee on Powder Diffraction Standards) to compare the crystal plans.

$$d = \frac{\lambda_{\text{Cu-}\alpha}}{2 * \sin(\theta)} \quad (1)$$

$$d_c = \frac{0.94 * \lambda_{\text{Cu-}\alpha}}{\beta * \cos(\theta)} \quad (2)$$

Where:  $\theta$  is the Bragg diffraction angle (°); and  $\beta$  is the full width at half maximum (FWHM).

The surface charge (Zeta potential) of the nanozeolites was determined by Doppler Light Scattering in Malvern-Zetasizer® equipment (model nano ZS, ZEN3600 - United Kingdom). The characteristics in aqueous media of samples such as Particle Hydrodynamic Diameter (PHd) and Polydispersity (Pd) were established by Dynamic Light Scattering DLS.

## 2.3. Experimental Design of Adsorption of AtL

The removal of AtL by adsorption was determined using a Central Composite Rotating Design (CCRD) (Table 1). In this sense, the independent variables used were nanozeolite concentration and pH of the AtL solution, where the percentage of AtL removal was the response variable.

Table 1. Independent variables used in CCRD 2<sup>2</sup>.

Level	[nSod] (g L <sup>-1</sup> )	pH
-1.41	0.33	2.75
-1.00	0.50	4.00
0	0.90	7.00
+1.00	1.30	10.00
+1.41	1.46	11.20

## 2.4. Adsorption Tests of AtL

The adsorption tests were performed in batch mode with the drug AtL [9]. In this sense, the samples were collected at predetermined times in 0 to 180 min, filtered with a 0.45  $\mu\text{m}$  pore filter, and the percentage of removal of the AtL dye (R, %) (Eq. 3) and the adsorption capacity ( $q_t$ , mg  $\text{g}^{-1}$ ) (Eq. 4) were determined using a UV-vis spectrophotometer (Varian Cary 100) at  $\lambda = 275$  nm.

$$R\% = \frac{C_0 - C_e}{C_0} * 100 \quad (4)$$

$$q_t = \frac{(C_0 - C_t) * V}{m} \quad (5)$$

Where:  $C_0$  is the initial concentration of the AtL (mg  $\text{L}^{-1}$ ) in  $t = 0$  min;  $C_t$  is the concentration of the AtL (mg  $\text{L}^{-1}$ ) in  $t = t$ ;  $V$  is the volume of the solution (L) and;  $m$  is the mass of the adsorbent (g).

## 2.5. Statistical Analysis

Experimental design was carried out using Statistic10 Software (version 10, Statsoft®, USA).

## 3. Results and Discussion

### 3.1. Characterization of the nanozeolites

The Figure 1(a) demonstrates the XRD diffractograms of the nanozeolites, where the samples presented the crystalline phases: nMeta demonstrated the Metahalloysite phase ( $\text{Al}_2\text{H}_4\text{O}_9\text{Si}_2$ , JCPDS n° 13-375, and  $d_c=29.81$  nm) at  $19.88^\circ$  (011,  $d=2.25$  Å),  $29.40^\circ$  (102,  $d=1.56$  Å),  $31.94^\circ$  (111,  $d=1.46$  Å),  $38.82^\circ$  (222,  $d=1.22$  Å),  $42.32^\circ$  (304,  $d=1.13$  Å), and  $50.17^\circ$  (502,  $d=0.99$  Å); nFau showed the Faujasite phase ( $\text{AlNaO}_{5.4}\text{Si}_{1.7}$ , JCPDS n° 12-0228, and  $d_c=14.22$  nm) at  $6.51^\circ$  (111,  $d=6.77$  Å),  $10.31^\circ$  (220,  $d=4.29$  Å),  $11.93^\circ$  (221,  $d=3.70$  Å),  $15.68^\circ$  (222,  $d=2.83$  Å),  $20.34^\circ$  (440,  $d=2.20$  Å),  $23.58^\circ$  (553,  $d=1.91$  Å),  $25.71^\circ$  (514,  $d=1.76$  Å), and  $30.32^\circ$  (555,  $d=1.53$  Å); nSod demonstrated the Sodalite phase ( $\text{C}_2\text{Al}_6\text{N}_2\text{Na}_{16}\text{O}_{24}\text{Si}_6$ , JCPDS no. 75-0709, and  $d_c=17.55$  nm) at  $14.06^\circ$  (110,  $d=3.15$  Å),  $19.78^\circ$  (101,  $d=2.26$  Å),  $24.39^\circ$  (200,  $d=1.85$  Å),  $31.58^\circ$  (211,  $d=1.47$  Å),  $34.67^\circ$  (220,  $d=1.35$  Å),  $37.61^\circ$  (002,  $d=1.25$  Å),  $42.77^\circ$  (202,  $d=1.12$  Å),  $52.04^\circ$  (321,  $d=0.92$  Å),  $58.32^\circ$  (411,  $d=0.90$  Å),  $62.17^\circ$  (103,  $d=0.86$  Å), and  $64.20^\circ$  (420,  $d=0.85$  Å) confirming the syntheses of the different zeolite phases. Moreover, the nanozeolites presented different Si/Al ratio indicating that decreasing the percentage of Si increment the removal of organic pollutants by adsorption [10].

The Table 2 shows the surface properties of the nanozeolites, where all samples presented a negative surface charge suggesting that the removal of AtL by the adsorption at ambient temperature and normal pH (around 7) will have result in electrostatic repulsion. It is worth mentioning that the PHd, and Pd values indicated overestimated values due to the dissolution of clays in the solvent associated with the composition of the zeolites generally containing silicon, aluminum, and sodium oxides.

Table 2. Surface Properties of Samples.

Samples	ZP (mV)	PHd (nm)	Pd
nMeta	$-24.6 \pm$	$1822 \pm$	$0.47 \pm$
	6.09	355	0.04
nFau	$-26.4 \pm$	$2245 \pm$	$0.57 \pm$
	2.70	415	0.04
nSod	$-18.8 \pm$	$947 \pm 118$	$0.37 \pm$
	6.85		0.03
Atenolol (298.1 K)	$-4.69 \pm$	$437 \pm 112$	$0.25 \pm$
	1.45		0.04

### 3.2. Adsorption of AtL

The Figure 1(b) demonstrates the initial results of AtL adsorption on nanozeolites. In this way, the nSod presented the removal of AtL of 82.5% compared to activated carbon of 42.8%. Therefore, based on the initial results of AtL adsorption the nSod was chosen for a study of different concentrations and pH of the solution.

The Pareto chart (Figure 1c) showed that the linear of 22 and quadric of 9.3 terms of nSOD were positives for AtL removal due to the increase in the number of active sites of the adsorbent for AtL molecules [11]. Furthermore, the quadratic pH variable of 17.8 induced an increase in AtL removal due to the change in the surface charge of AtL related to the  $\text{pK}_a$  of Atenolol of 9.8 increasing the electrostatic interactions with nSod and facilitating the drug dissolution at extreme pHs (<2) and (>10). In this sense, Figure 1(d) presents the 2D response surface, where the increase in [nSod] and the extreme pH values is evident in the removal of AtL. Figure 1e presents the kinetic models tested for the adsorption data of AtL, where the pseudo-second-order model best fitted the data ( $q_e=28.68$  g  $\text{mg}^{-1}$  g<sup>-1</sup>) indicating the formation of chemical bonds involving the exchange or donation of electrons between the adsorbate and the adsorbent, with the adsorption rate being proportional to the square of the number of active sites on the adsorbate surface.

## 4. Conclusion

In this work, it was possible to synthesize nanostructured zeolites with different phases from (agro)industrial waste. Moreover, the nSod was effective in the removal of AtL, where the variables adsorbent concentration and pH influenced and optimized the removal. Therefore, nSod can be effectively used for the adsorption of the organic pollutant Atenolol correlating topics of environment, sustainability, and nanotechnology.

## Acknowledgements

The authors would like to thank the Applied Nanomaterials Research Group (GPNap) and Franciscan University (UFN) for the support and assistance to carry out the present work. This study was financed in part by the Coordenação de Aperfeiçoamento de Pessoal de Nível Superior – Brasil (CAPES) – Finance Code 001.

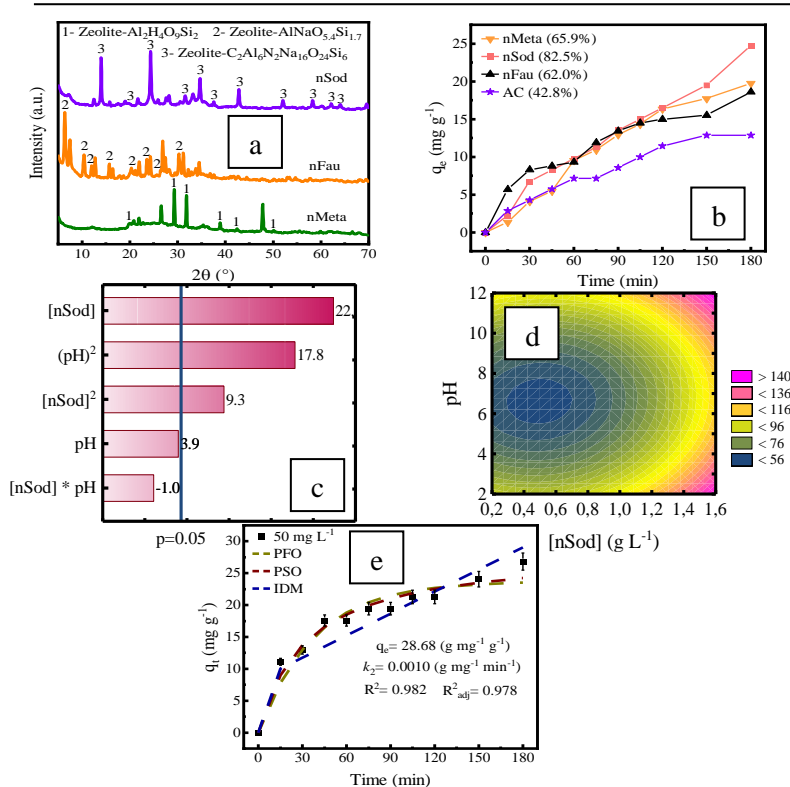


Figure 1. (a) Diffractograms; (b) Adsorption initial tests of AtL containing Zeolites; (c) Pareto Chart; (d) 2D-Surface using nSod as adsorbent; and (e) Kinetic study of adsorption.

## References

- [1] Adeola AO, Forbes PBC. Advances in water treatment technologies for removal of polycyclic aromatic hydrocarbons: Existing concepts, emerging trends, and future prospect. *Water Res* 2021;293: 343-59.
- [2] Rosero HG, Cano LAR, Aguilar A, García EB, Carvalho AP, Cadenas AFP, Marín FC. Adsorption and thermal degradation of Atenolol using carbon materials: Towards an advanced and sustainable drinking water treatment. *J Water Process Eng* 2022;49:102987-996.
- [3] Zhou S, Di-Paolo C, Wu X, Shao Y, Seiler T, Hollert H. Optimization of screening-level risk assessment and priority selection of emerging pollutants – The case of pharmaceuticals in European surface waters. *Environ Int* 2019;1:1-10.
- [4] Hu Y, Fitzgerald NM, Lv G, Xing X, Jiang WT, Li Z. Adsorption of Atenolol on Kaolinite. *Adv Mater Sci Eng* 2015;2015:897870-879.
- [5] Oviedo LR, Muraro PCL, Chuy G, Vizzotto BS, Pavoski G, Espinosa DCR, Rhoden CRB, Da Silva WL. Antibacterial activity of nanozeolite doped with silver and titanium nanoparticles. *J Solgel Sci Technol* 2022;101:235-43.
- [6] Lian S, Fan S, Yang Y, Yu B, Dai C, Qu Y. Selenium nanoparticles with photocatalytic properties synthesized by residual activated sludge. *Sci Total Environ* 2022;809:151163-170.
- [7] Miao S, She P, Chang X, Zhao C, Sun Y, Lei Z, Sun S, Zhang W, Jia M. Synthesis of beta nanozeolite aggregates with hierarchical pores via steam-assisted conversion of dry gel and their catalytic properties for Friedel-Crafts acylation. *Microporous Mesoporous Mater* 2022;334:111777-792.
- [8] Oviedo LR, Druzian DM, Montagner GE, Ruiz YPM, Galembeck A, Pavoski G, Espinosa DCR, Nora LDD, Da Silva WL. Supported heterogeneous catalyst of the copper oxide nanoparticles and nanozeolite for binary dyes mixture degradation: Machine learning and experimental design. *J Mol Liq* 2024;402:124763-781.
- [9] Salgado R, Pereira VJ, Carvalho G, Soeiro R, Gaffney V, Almeida C, Cardoso V, Ferreira E, Benoliel MJ, Ternes TA, Oehmen A, Reis MAM, Noronha JP. Photodegradation kinetics and transformation products of ketoprofen, diclofenac and atenolol in pure water and treated wastewater. *J Hazard Mater* 2013;244-245:516-27.
- [10] Jiang N, Shang R, Heijman SGJ, Rietveld LC. High-silica zeolites for adsorption of organic micropollutants in water treatment: A review. *Water Res* 2018;144:145-61.
- [11] Haro NK, Vecchio PD, Marcilio NR, Féris LA. Removal of atenolol by adsorption – Study of kinetics and equilibrium. *J Clean Prod* 2017;154:214-19.